

Figure S1

A.

Macrophage clusters:

- 1 Macrophage
- 2 Macrophage
- 4 Macrophage

Endothelial clusters:

- 3 Endothelial
- 5 Endothelial

Dendritic cell cluster:

- 7 Dendritic cell

Pericyte/ Smooth muscle cluster:

- 9 Pericyte/Smooth Muscle
- 11 Pericyte/Smooth Muscle

Lymphocyte cluster:

- 10 Lymphocyte

Neuro-muscular cluster:

- 12 Neuro-Muscular

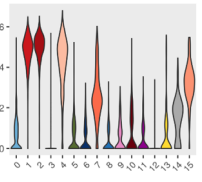
Nerve cluster:

- 13 Nerve

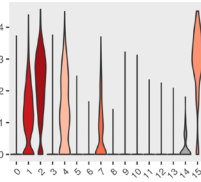
Granulocyte cluster:

- 15 Granulocyte

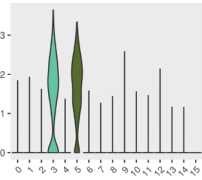
Lyz2



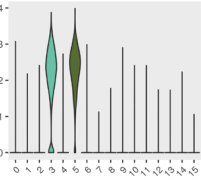
Cd14



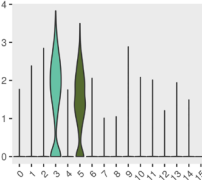
Emcn



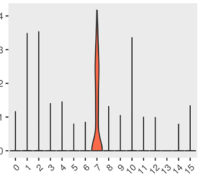
Pecam1



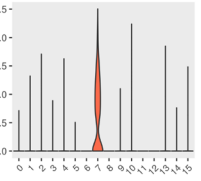
Sox18



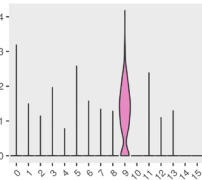
Cd209a



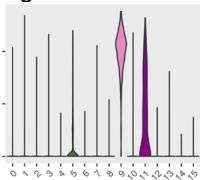
Flt3



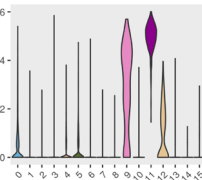
Abcc9



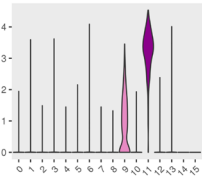
Rgs5



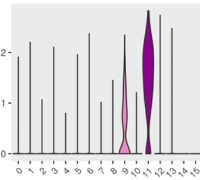
Acta2



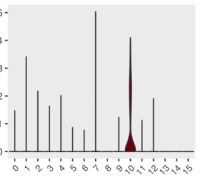
Myh11



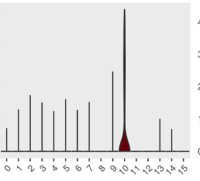
Pde3a



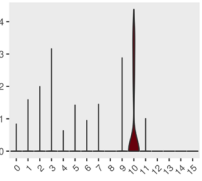
Ccr7



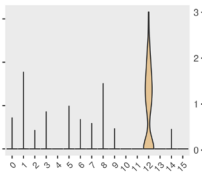
Ms4a4b



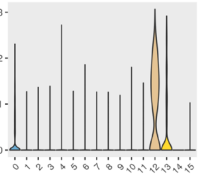
Ms4a1



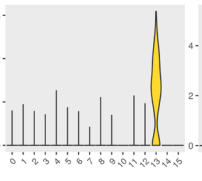
Pax7



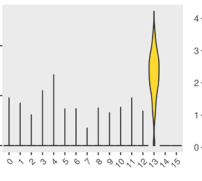
Ncam1



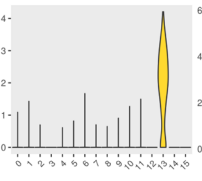
Sox10



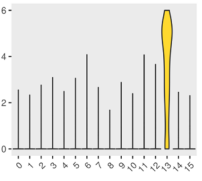
Plp1



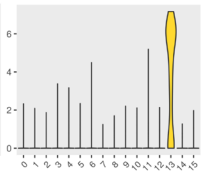
Kcna1



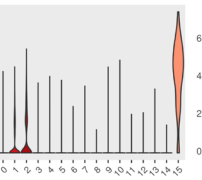
Mbp



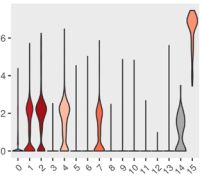
Mpz



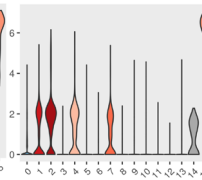
Csf3r



S100a8



S100a9



Cxcr2

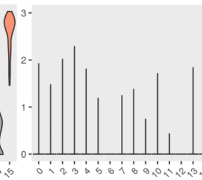


Figure S1 cont.

B

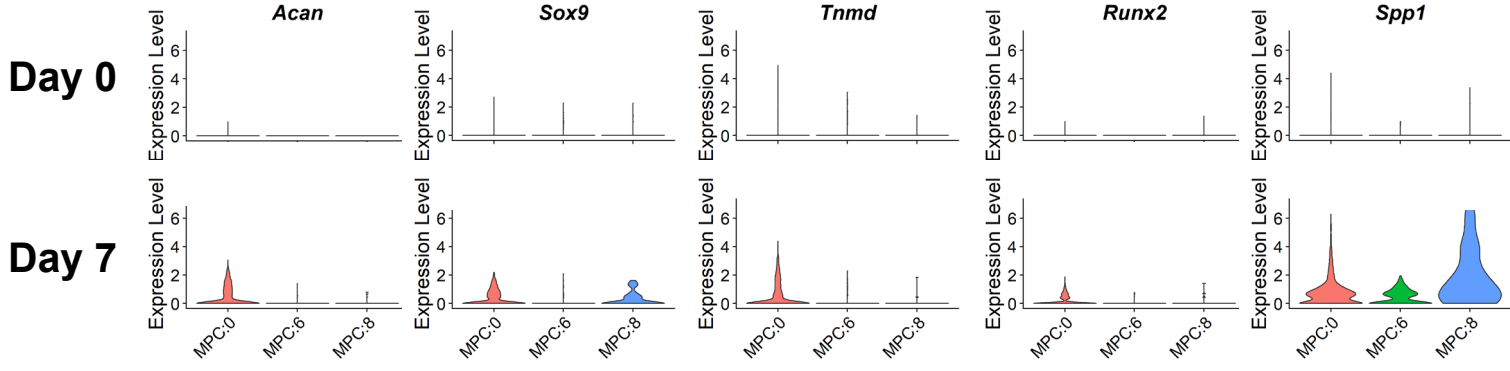


Figure S1 cont.

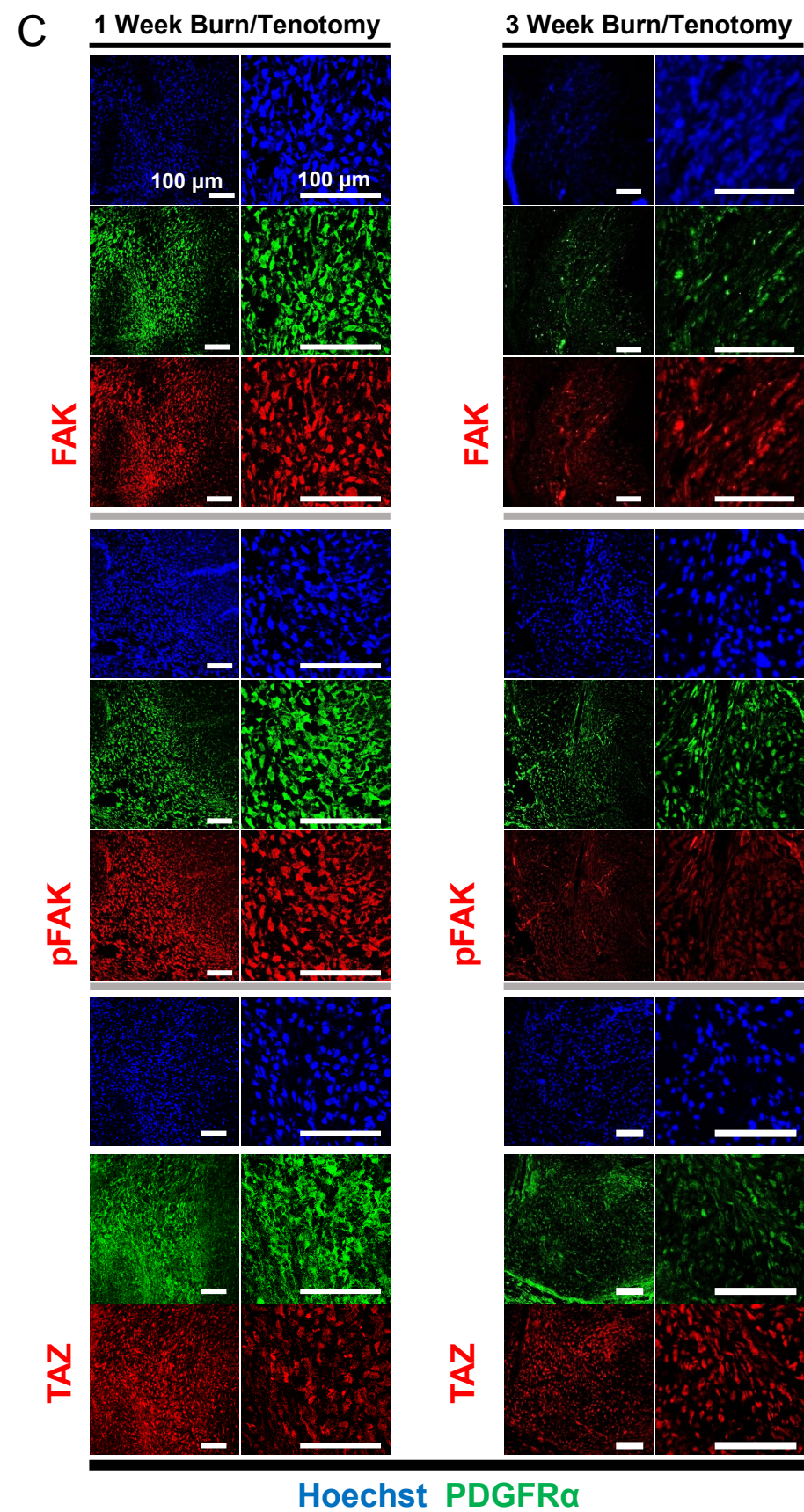


Figure S1. (A) Gene expression defining clusters of day 0, 3, 7, and 21 canonical correlation analysis, MPC differentiation genes, and individual channels of confocal microscopy images. (B) Violin plots of differentiation associated genes in each of the MPC cell clusters. (C) Individual channels of FAK, pFAK, and TAZ from Figure 1E and F.

Figure S2

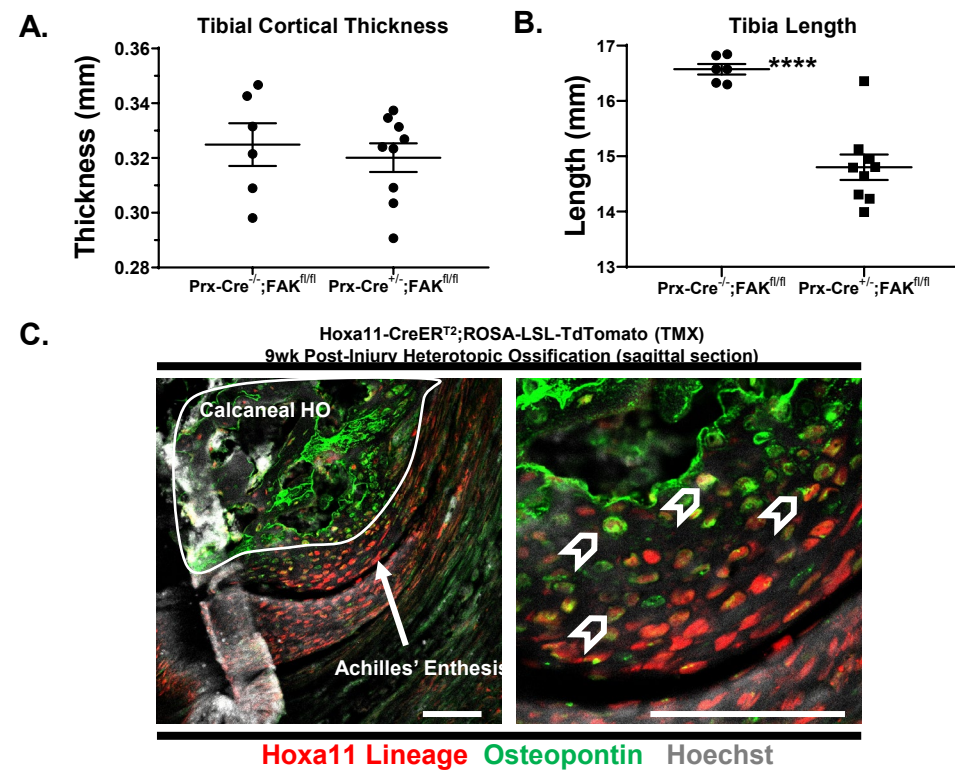
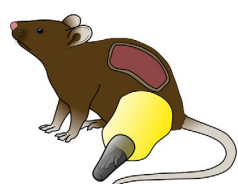


Figure S2. (A) Tibial cortical thickness and (B) length in PrxCre^{-/-};FAK^{fl/fl} and PrxCre^{+/-};FAK^{fl/fl} mice. (C) Confocal images of the HO site in Hoxa11CreER;R26TdTomato reporter mice 9 weeks after injury.

Figure S3

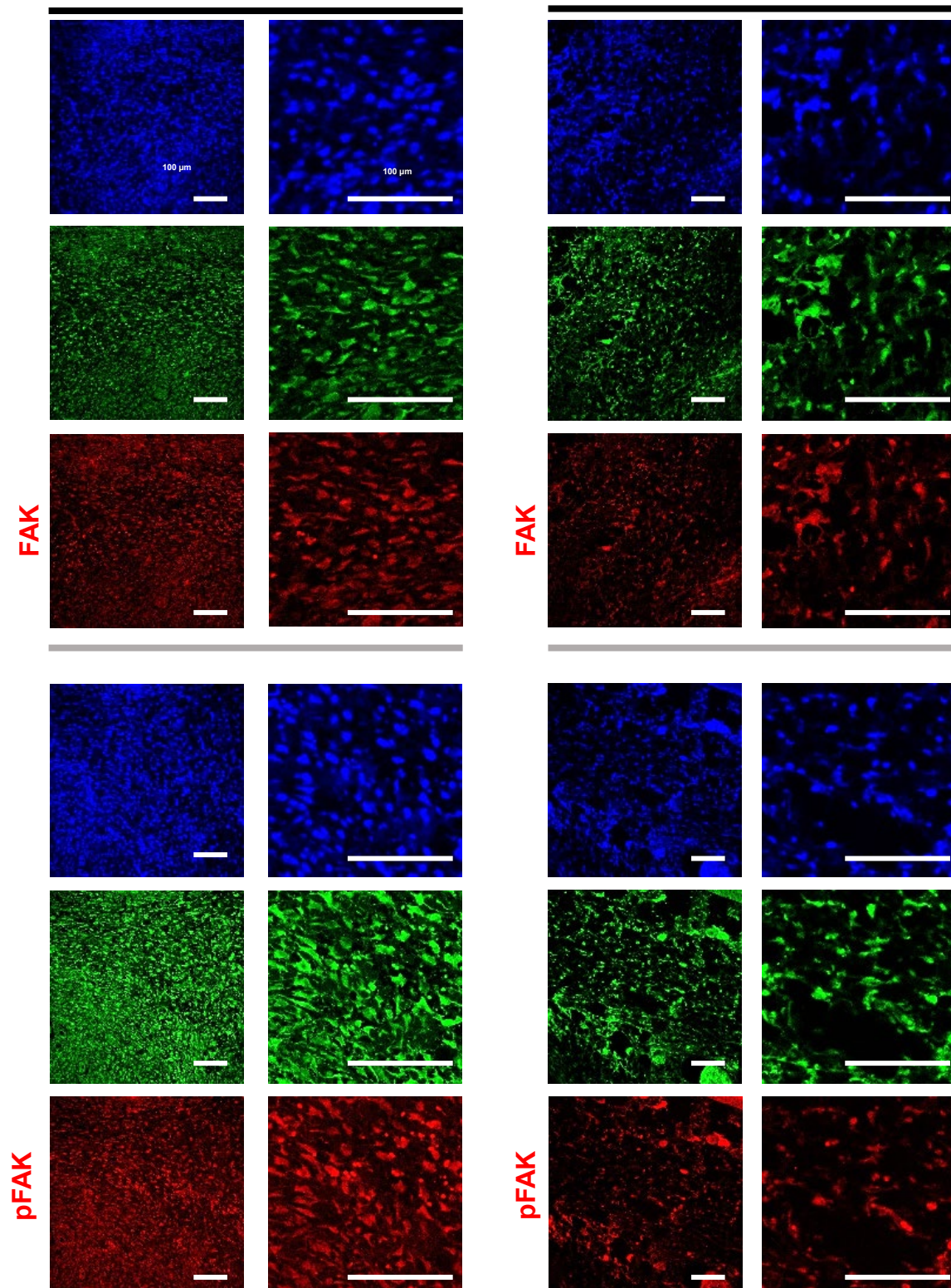
A.



B.

1 Week Mobilized

1 Week Immobilized



Hoechst PDGFR α

Figure S3 Cont.

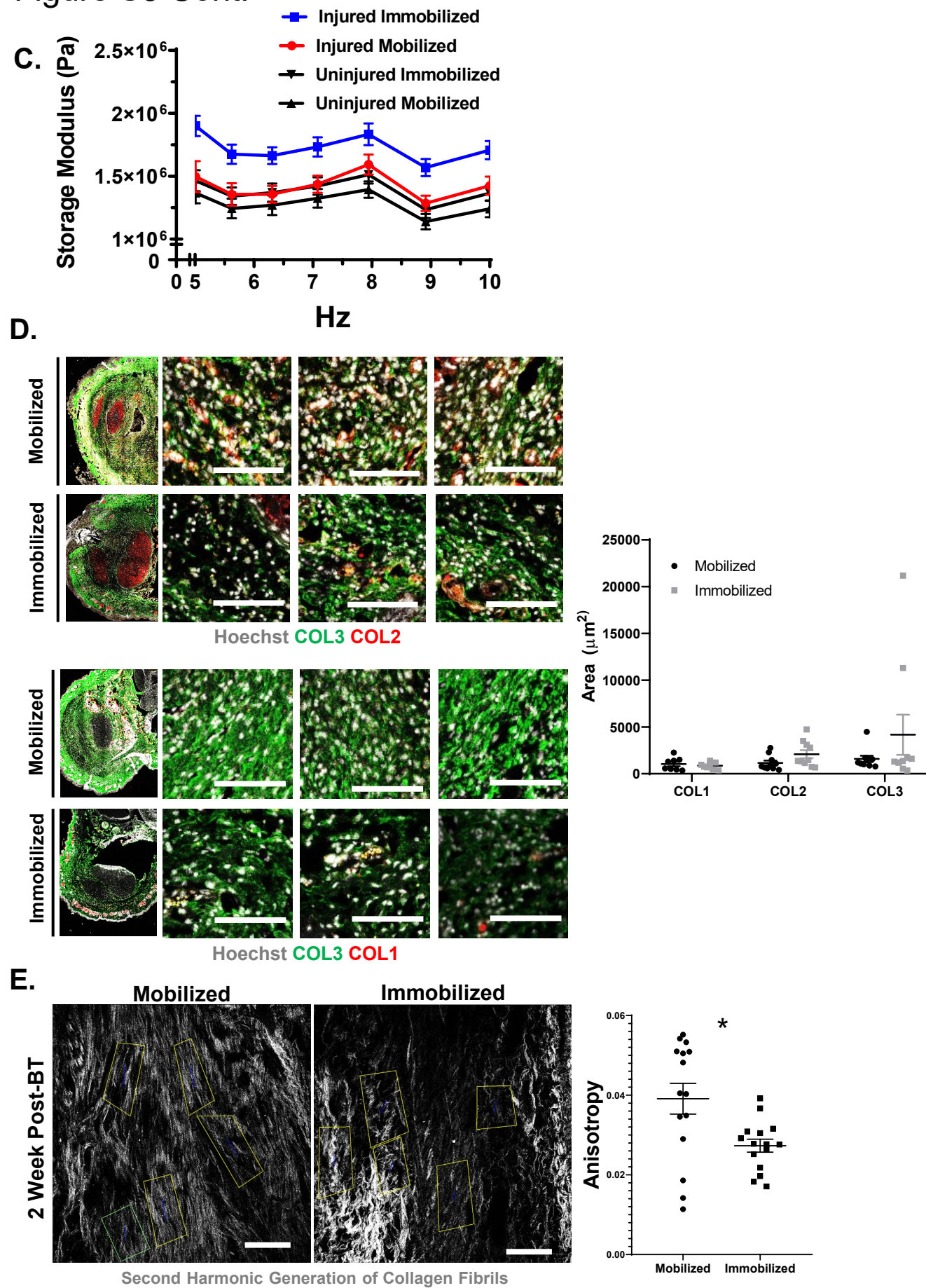


Figure S3. (A) Joint immobilization model. (B) Individual channels of FAK, pFAK and TAZ from Figure 3B. (C) DMA analysis of mobile and immobile mice. (D) Staining of Col1, Col2, and Col3 in mobile and immobile mice. (E) SHG and tissue alignment of the ECM in mobile and immobile mice 2 weeks post B/T.

Figure S4

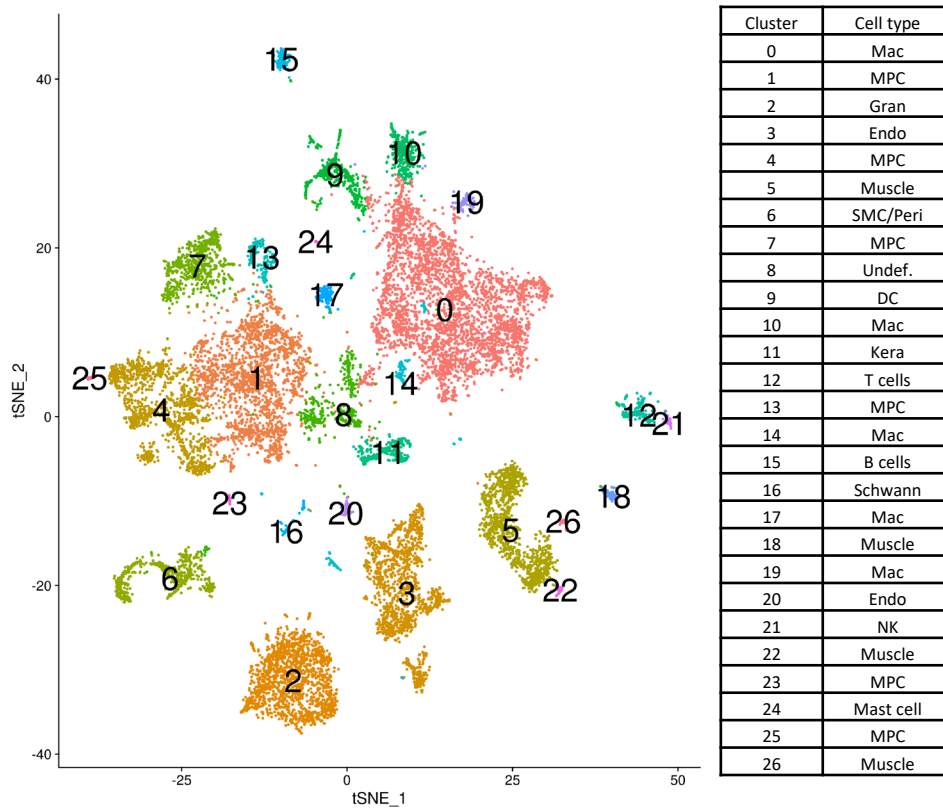


Figure S4. tSNE of day 0, day 7 mob, and day 7 immob scRNA-seq. Canonical cluster identified 27 unique clusters that were classified based on their gene expression.

Table S1. Adipogenic and osteogenic signature genes.

Adipogenic genes	Osteogenic genes
<p><i>Lmna, Egr2, Adrb2, Lrp5, Agt, Rxra, Dkk1, Cebpa, Adipoq, Fasn, Lipe, Cdk4, E2f1, Prdm16, Ppara, Cdkn1b, Cdkn1a, Klf2, Ncor2, Fabp4, Ucp1, Pparg, Dio2, Src, Axin1, Wnt1, Klf4, Lpl, Wnt3a, Cfd, Ncoa2, Slc2a4, Irs1, Runx1t1, Foxc2, Nr0b2, Nr1h3, Foxo1, Klf15, Hes1, Cebpb, Taz, Insr, Sirt2, Vdr, Ddit3, Ccnd1, Dlk1, Creb1, Klf3, Ppargc1b, Acacb, Fgf10, Fgf1, Sirt3, Irs2, Tcf7l2, Nrfl, Ppargc1a, Gata2, Mapk14, Jun, Rb1, Lep, Ppard, Srebf1, Sfrp1, Wnt5b, Gata3, Cebpd, Angpt2, Sirt1, Retn, Tsc22d3, Adig, Sfrp5, Mtor, Ucp2, Tfam, Zfp423, Cd34, Itgb1,</i></p>	<p><i>Spp1, Bgn, Tgfb1, Bmp1, Csf2, Tgfb3, Gdf10, Mmp10, Sox9, Comp, Csf3, Smad2, Col4a1, Igf1r, Smad3, Vegfa, Alpl, Smad4, Vegfb, Tgfb2, Dlx5, Vcam1, Cdh11, Cd36, Bmp3, Runx2, Acvr1, Itgav, Csf1, Anxa5, Col2a1, Ihh, Flt1, Pdgfa, Phex, Serpinh1, Tnf, Itga2, Tgfb2, Mmp9, Bmpr2, Fgfr2, Chrd, Col5a1, Mmp8, Itga2b, Bmpr1b, Bmpr1a, Nog, Icam1, Col3a1, Igf1, Egf, Itga3, Tgfb3, Nfkb1, Bmp5, Bglap, Fn1, Colla1, Ctsk, Fgfr1, Bmp6, Tgfb1, Ahsg, Col10a1, Smad1, Itgam, Sp7, Sost, Smad5, Col1a2, Col14a1, Gli1, Tnfsf11, Plcb4, Akt3, Alcam, Cdh2, Met, Ptpnf, Tns1, Greml, Col12a1, Fbn1, Ibsp, Igf2, Pdlim7, Postn, Sparc, Cav2, Itga7, Ptk2, Dkk3, Serpine1, Thbs1, Fzd6, Jag1, Egfr, Prepl, Col8a1, Itga11, Ptpn14, Thbs3, Bdnf, Lepr, Pcolce, Spock1, Pafah1b1, Pgf, Tbx3, Fgfr1, Timp3, Fzd8, Tnfrsf11b, Ccl2, Tle1, Col15a1, Igfbp2, Efnb2, Anxa5, Alcam, Twist1, Fgf2, Bmp2, Bmp4, Bmp7, Wnt5a, Thbs4</i></p>

Table S2: List of antibodies and dilutions.

Antibody/Chemical	Product #	Clone	IF Dilution	ICC Dilution	WB
anti-FAK	CST3285	polyclonal	1:50		
anti-pFAK	inv44-626G	polyclonal	1:50	1:200	
anti-PDGFRa	AF1062	polyclonal	1:25		
anti-TAZ	NB110-58359	polyclonal	1:50	1:200	
anti-pSMAD3	NBP1-77836	polyclonal	1:50		
anti-pSMAD2	CST 3108	138D4			1:800
anti-SMAD2	CST 5339	D43B4			1:1000
anti-Gapdh	CST 5174	D16H11			1:1000
anti-Perilipin-1	CST 9349	D1D8	1:50		
anti-Collagen 1	ab34710	polyclonal	1:50		
anti-Collagen 2	ab34712	polyclonal	1:50		
anti-Collagen 3	NBP1-26547	polyclonal	1:50		
anti-Sox9	ab185230	EPR14335	1:50		
anti-PPARg	16643-1-AP	polyclonal			1:800
anti-Vinculin	V9264	hVIN-1	1:500		
Goat anti-mouse AlexaFluor-647	A21235		1:1000		
Donkey anti-goat AlexaFluor-488	A11055				
Donkey anti-goat AlexaFluor-594	A32758				
Donkey anti-rabbit AlexaFluor-488	A21206				
Donkey anti-rabbit AlexaFluor-594	A21207				
Donkey anti-rabbit AlexaFluor-647	A31573			1:250	
Anti-rabbit IgG, HRP linked	CST7074				1:3000
Phalloidin AlexFluor-488	Ab176753			1:1000	
Hoechst 33342	H3570		1:2000	1:500	
BODIPY-493/503	D3922			1:1000	

Movie S1. MPC migration on aligned and non-aligned functionalized synthetic fibrous matrices.

Supplement

Burn/Tenotomy HO Model (Cont.)

Briefly, mice were anesthetized with inhaled isoflurane. Dorsal hair was closely clipped, and an aluminum block heated to 60°C was exposed to the dorsal region over 30% of the total body surface area for 18 seconds to achieve a partial-thickness burn injury. Each mouse then received a concurrent sterile dorsal hind limb tendon transection at the midpoint of the Achilles tendon (Achilles tenotomy) with placement of a single 5-0 vicryl suture to close the skin. Pain management was achieved with subcutaneous injections of buprenorphine (Buprenex, Reckitt Benckiser Pharmaceuticals) every 12 hours for 2 days.

Single Cell RNA Sequencing using 10X Genomics (1)

Day 0 and post-surgery day 3, 7, and 21 harvested tissue samples were digested for 45 minutes in 750U/ml Type 1 Collagenase and 7U/ml Dispase II (Gibco) in Roswell Park Memorial Institute (RPMI) medium at 37°C under constant agitation at 180 rpm. Digestions were subsequently quenched with 2% FBS in PBS and filtered through 40µm sterile strainers. Cells were then washed in 2% FBS in PBS, counted and resuspended at a concentration of 1000-1200 cells/ul. Cell viability was assessed with Trypan blue exclusion on a Countess II (Thermo Fisher Scientific) automated counter and only samples with >85% viability were processed for further sequencing.

Single-cell 3' library generation was performed on the 10x Genomics Chromium Controller following the manufacturers protocol for the v3.1 reagent kit (10X Genomics, Pleasanton, CA, USA). Cell suspensions were loaded onto a Chromium Single-Cell G chip along with reverse transcription (RT) master mix and single cell 3' gel beads, aiming for 2000-6000 cells per channel. In this experiment, 8700 cells were encapsulated into emulsion droplets at a concentration of 700-1200 cells/ul which targets 5000 single cells with an expected multiplet rate of 3.9%. Following generation of single-cell gel bead-in-emulsions (GEMs), reverse transcription was performed, and the resulting Post GEM-RT product was

cleaned up using DynaBeads MyOne Silane beads (ThermoFisher Scientific, Waltham, MA, USA). The cDNA was amplified, SPRIselect (Beckman Coulter, Brea, CA, USA) cleaned and quantified then enzymatically fragmented and size selected using SPRIselect beads to optimize the cDNA amplicon size prior to library construction. An additional round of double-sided SPRI bead cleanup is performed after end repair and A-tailing. Another single-sided cleanup is done after adapter ligation. Indexes were added during PCR amplification and a final double-sided SPRI cleanup was performed. Libraries were quantified by Kapa qPCR for Illumina Adapters (Roche) and size was determined by Agilent tapestation D1000 tapes. Read 1 primer sequence are added to the molecules during GEM incubation. P5, P7 and sample index and read 2 primer sequence are added during library construction via end repair, A-tailing, adaptor ligation and PCR. Libraries were generated with unique sample indices (SI) for each sample. Libraries from days 0, 3, 7, and 21 were sequenced on a HiSeq 4000, (Illumina, San Diego, CA, USA) using a HiSeq 4000 PE Cluster Kit (PN PE-410-1001) with HiSeq 4000 SBS Kit (100 cycles, PN FC-410-1002) reagents, loaded at 200 pM following Illumina's denaturing and dilution recommendations.

Bioinformatics Analysis of Single Cell Sequencing Data

Multiple Time Point Analysis

Replicates from days 0, 3, 7, and 21 were selected in order to have a balanced number of cells per time point. Replicates 1-4 for day 0 (3815 cells), replicates 1-2 for day 3 (4201 cells), replicate 1 for day 7 (3405 cells), and replicates 1-3 for day 21 (3505 cells) were used. The sequencing data were first preprocessed with 10x Genomics software Cell Ranger (10x Genomics Inc., Pleasanton, CA, USA), and aligned to mm10 genome. Downstream analysis was performed with Seurat 2.3.0 (2). For quality control, cells were pooled together from all the time points. Genes expressed in more than 10 cells in this pooled set were kept (17131 genes). Cells with total expressed genes in the range of [500, 5000], and fraction of mitochondrial gene UMIs lower than 0.2, were retained (3495 cells for day 0, 3573 cells for day 3, 3132 cells for day 7, and 3162 cells for day 21). Filtered samples were processed as Seurat objects. Counts were normalized (default Seurat parameters) and scaled (regressing against number of genes expressed

per cell and fraction of mitochondrial expression). Variable genes were extracted (default Seurat parameters). Overall variable genes were defined as the intersection of the top 5000 genes for each replicate (1497 genes). Replicates were joined via canonical correlation analysis (20 components, using the overall variable genes). Unsupervised clustering was used to find the cell communities (Louvain algorithm, resolution 0.4, using the aligned canonical correlation components), leading to 16 clusters, numbered 0 to 15. Clusters were labeled according to characteristic genes (Figure S1A). Markers were calculated with FindMarkers and ranked according to the difference in the fractions of cells expressing each marker within cluster versus the rest of the considered cells. Marker enrichment was obtained with iPathway (3).

Assay of Transposase Accessible Chromatin (ATAC)-sequencing

ATAC-Seq libraries were prepared at the UM Epigenomics Core by using the Omni-ATAC protocol for cells as described in Corces et al., 2017 without modifications (4). We used a custom pipeline designed with Snakemake to perform the bioinformatics analysis for ATAC-Seq samples. Quality of reads were checked with FastQC. Reads were trimmed using Trim Galore! and Nextera transposase adapters. Inspection with FastQC (and MultiQC) after before/after trimming indicates this was successful. Trimmed reads were aligned to the mm10 genome using bowtie2 with additional flags which are often used in ATAC-seq (-X 2000 --no-mixed --no-discordant). Alignment rates were 75% - 80% of reads aligning uniquely. Duplicates (optical and PCR) were removed from initial alignments with Picard. Alignments on chrM and with MAPQ < 10 were removed. Alignments falling in ENCODE blacklist sites were removed. MultiQC was run and summarizes the QC steps. BigWig files were created for viewing of read pile-ups in genome browser. Macs2 with -f BAM --nomodel --shift -100 --extsize 200 were run resulting in the following number of peaks each: 49,680 for day 0, 68,191 for day 7 immobile, and 46,247 in the day 7 mobile MPCs. All peaks were then merged together. Number of reads from each sample that fell inside the merged peaks were counted. These tables were read into edgeR, and then we performed 3 tests. Because samples from multiple mice were pooled, and there was only one replicate per condition,

we used a fixed Biological Coefficient of Variation of 0.21. A FDR < 0.05 threshold for significance was used. For analysis, open chromatin regions were identified using F-Seq (5) and annotated using ChIPseeker (6).

Day 7 Mobile vs. Immobile Analysis

Burn and tenotomy was performed on *Hoxa11*CreER;R26^{TdTomato} mice. Mice were either allowed to ambulate normally or were immobilized for 7 days. Tissue was harvested from the tenotomy injury site and processed to obtain heterogeneous cell suspensions as described above. Single cell 3' sequencing and single cell ATAC sequencing was performed on day 0 (naïve), day 7 mobile, and day 7 immobile samples. Library generation was performed using the 10x Genomics Chromium GEM Single Cell 3' Reagents kit v3.1 following the manufacturer's protocol. Sequencing was performed on the NovaSeq 6000 (Illumina, San Diego, CA, USA) S4 flowcell 300 cycle kit. This was loaded in order to target 500M reads/sample (5000 cells, 100K reads/cell), at 300pM (these were shared flowcells). The read length configuration was 150 x 8 x 150 cycles for Read 1, Index and Read 2, respectively. Cell Ranger Single Cell Software Suite 1.3 was used to perform sample de-multiplexing, barcode processing, and single cell gene counting (Alignment, Barcoding and UMI Count) at the University of Michigan Biomedical Core Facilities DNA Sequencing Core. For single ATAC sequencing, libraries were generated using the 10X Chromium Next GEM Single Cell ATAC kit v1.1; Chemistry with NextGEM Chip H. The sequencing was performed on the NovaSeq 6000 using the SP flowcell 100 cycle kit. Read lengths: 50 x 8 x 16 x 49.

A different data set was generated to compare mobile and immobile replicates. We considered three replicates for day 7 immobile, one replicate for day 7 mobile, and one replicate for day 0. Seurat 3.1.1 (2) was used for downstream analysis. Cells with total expressed genes in the range of [500, 5000], or [500, 7500], depending on the replicate, were retained. Cells with a fraction of mitochondrial gene UMIs higher than 0.25 were discarded. Filtered replicates (878 cells for day 0; 3007, 3240, and 3904 cells for day 7 immobile; and 4174 cells for day 7 mobile) were processed as Seurat objects. Replicates were integrated according to the standard Seurat 3 workflow. Counts were normalized and variable genes were

calculated (vst method) on each single replicate. The first 100 dimensions were considered for both finding integration anchors and integrate the replicates. The integrated set was then scaled, regressing out cell cycle scores, number of genes per cell, number of counts per cells, and fraction of the mitochondrial gene UMIs. Unsupervised clustering was applied to the integrated set to find the cell communities (Louvain algorithm, resolution 0.3, using the aligned canonical correlation components), leading to 27 provisional clusters (Figure S4). Markers for each provisional cluster were calculated with FindMarkers and ranked according to the difference in the fractions of cells expressing each marker within cluster versus the rest of the considered cells. Provisional clusters were labeled as cell type according to characteristics genes. Clusters that were labeled with common cell types were condensed to give 14 clusters (Figure 5A). After this, gene expression from the MPC defined clusters were used to align the scATAC sequencing data using Signac 3.1.5. Briefly, scATAC data from the three conditions - day 0, day 7 immobile and day 7 mobile were merged after limiting the dataset to those cells that have at least 100 features. The resulting combined Seurat object was then normalized using default parameters and top variable features (peak accessibility) using a minimum cutoff of 20 cells were calculated. Dimension reduction was done using t-SNE using dimensions 2 through 30 as input features. Unique clusters were determined using a shared nearest neighbor modularity optimization-based clustering algorithm with a resolution of 0.2. scRNA-seq data was used to guide the cluster labeling using `cca` reduction using the FindTransferAnchors function. This resulted in 6 cell-type based clusters in the scATAC data. The MPC cluster of cells was isolated, and another round of unsupervised clustering was done to obtain 5 sub-clusters. Top differentially accessible marker genes were then identified in each of these sub-clusters using FindAllMarkers with a log fold-change threshold of 0.25.

Cell Trajectories

Cell trajectories were calculated with Monocle 2.13.0 (7), based on the top 1000 overall variable genes, ranked by scaled dispersion, obtained from Seurat.

Adipogenic Score

The adipogenic score was calculated as follows. First, a list of adipogenic and osteogenic genes was obtained from literature. These were hand selected by using genes (Table S2) that were in Adipogenesis and Osteogenesis RT2 profiler panels (Qiagen) as well as genes obtained from various publications that included adipogenic and osteogenic genes (8-11). Gene lists were hand selected, omitting overlapping genes. Genes that were not expressed in the joined day 7 mobile versus immobile set were filtered out, leaving an adipogenic and osteogenic signatures of, respectively, 82 genes and 129 genes. The combination of the signature was utilized as the adipogenic score probe vector, with 82 values corresponding to the adipogenic genes set to 1, and the 129 values corresponding to the osteogenic genes set to -1. For each cell, the score is calculated as the rank (Spearman) correlation between the probe vector and the cell gene expression profile (in UMIs) for the same genes.

Dynamic Mechanical Analysis

Briefly, 8mm³ of tissue was excised from each tendon insertion (HO) site in injured and uninjured tendons (n=10 mice/group). Each sample was centered in a spherical depression before lowering a probe onto the sample with a 0.05N preload. Next, a 1% oscillatory strain was applied and the storage modulus (based on the cross-sectional area of the probe) was measured over a frequency range of 0.2–1.0 Hz. Significance was measured by two-way ANOVA.

Oil Red O

Optimal Cutting Temperature Compound (OCT) was washed off cryosections with 1X PBS. Sections were washed in 60% isopropanol then stained in 3 mg/mL Oil Red O solution (O0625-25G, Sigma-Aldrich) for 15 minutes. Samples were washed with 60% isopropanol and nuclei counterstained with Haematoxylin (GHS316-500ML, Sigma-Aldrich) then washed in water. Sections mounted with AquaMount (#13800, Lerner Laboratories) and imaged on Olympus BX51 upright microscope. Regions of interested were color transformed to YIQ and threshold set using 2/3 channel for all images in ImageJ

(<https://imagej.nih.gov/ij/plugins/color-transforms.html>). Percent area measured and statistical analysis performed in Prism 8.

Immunofluorescence Histology

Hindlimbs were harvested at various time points, fixed in 4% paraformaldehyde for 24 hours, imbedded in OCT, and cross-sectioned at 10 μ m thickness onto glass slides. Sections were washed in 0.05% TBST, blocked in Donkey blocking media for 2 hours, and incubated with primary antibody overnight at 4°C at designated dilution (Table S2). Primary antibody was washed off with 0.05% TBST and incubated for 2 hours with secondary antibody at 1:200 dilution. Slides were stained with nuclear Hoechst 3342 stain for 5 minutes. Slides were mounted with Prolong Glass Mounting Media (P36980, Invitrogen) and imaged using Leica SPX8 Confocal Scanning Microscope.

Immunocytochemistry (ICC)

Cells were washed with 1X PBS then fixed in 4% PFA for 15 minutes. Cells were permeabilized for 5 minutes with 1X TBS 0.5% Triton X-100. Cells incubated overnight at 4°C in 10% donkey blocking solution (percent donkey serum in 1X TBS 0.5% Triton X-100). Cells were washed twice with 1X PBS and primary antibodies were added in a 2% Blocking solution in 1X TBS 1% Triton X-100. Antibody dilutions are indicated in (Table S1). Cells were washed 3 times in 1X PBS. Secondary antibodies were added in 2% ICC blocking solution and incubated for 1 hour at room temperature; dilutions indicated in (Table S1). Cells were then incubated in Hoechst 33342 for 15 minutes, washed, and then mounted on glass slides with prolong glass. For vinculin immunostaining, samples were simultaneously fixed and permeabilized in 0.5% paraformaldehyde in microtubule-stabilizing buffer for 15 min at room temperature to extract cytoplasmic vinculin. Samples were then blocked for 1 h in 10% fetal bovine serum, incubated for 1 hour with primary mouse monoclonal anti-vinculin, and incubated for 1 hour with secondary AlexaFluor 647 goat anti-mouse sequentially at room temperature. AlexaFluor 488 phalloidin and 4',6-diamidino-2-phenylindole were utilized to visualize F-actin and nucleus, respectively. Slides were imaged on Leica SPX8 Confocal Scanning Microscope.

Western Blot

Tissue was homogenized with a mortar and pestle. Cells were lysed with RIPA buffer lysis system (sc-24948A, Santa Cruz Biotechnology) and assessed for total protein using Pierce BCA Protein Assay Kit (cat #. 23225). Proteins from lysate were separated on NuPAGE™ 4-12% bis-tris Gel (NP0335BOX, Invitrogen) with NuPAGE™ SDS running buffer (NP0001, Invitrogen). Protein was transferred to PVDF membrane (IPVH00010, Millipore Sigma) in NuPAGE™ transfer buffer (NP0006, Invitrogen). Membrane was washed in wash buffer (1X TBS 0.05% Tween-20) and then incubated at room temperature in 5% milk protein in wash buffer (block solution) for 1 hour. Membrane was then incubated with primary antibody diluted in 5% BSA in wash buffer. The appropriate HRP linked secondary was diluted in block solution. Antibody dilutions can be found in Table S1. FIJI and excel were used for quantification.

X-Ray Imaging

Mouse hindlimbs were imaged using Faxitron Mx20 machine. Images were taken at 3x magnification for 6 seconds at 25 kV. Film was processed using the Hope Micro-Max X-ray processor. Radiographs were digitally scanned and ectopic bone within tendon and around calcaneus was segmented by trained user. Area of heterotopic ossification was calculated and compared between groups.

MicroCT

Injured left legs were scanned by μ CT and bone volumes were determined (Bruker SkyScan 1176, 35 μ m resolution, 357 μ A beam energy, 70 kV beam current, 520 ms exposure). Scans were analyzed using calibrated imaging protocol as previously described by MicroView μ CT viewer (GE Health Care and Parallax Innovations) (12). Bone reconstructions were calculated at 800 HU depicting representative means of treatment groups. Ectopic bone was manually splined and measured at 800, and 1250 Hounsfield Unit (HU) thresholds. Ectopic bone volumes were characterized as total volume, proximal, distal, floating, and bone associated. Tibial cortical thickness was measured at 1250 HU over a

700-micron distance starting from 70 microns proximal to the tibia-fibula fuse point. Tibia Length was measured as well.

In Vitro and In Vivo Cell Quantifications

Multiple ROIs per section (n=2-5) were imaged by confocal microscopy for cell spread area and aspect ratio quantification to capture representative regions of tissue (n=2-4 mice/group) or culture substrates (n=3/group). Quantifications were performed in FIJI software (13). Cell aspect ratio was measured as by blinded operator by drawing length and width of cell in perpendicular fashion. Length was divided by width for aspect ratio measurement (n>10 cells/image). Cell area quantification was performed by blinded operators segmenting individual cells (n>10 cells/image) and using the triangle threshold in image J to determine positive signal. Lipid droplet quantification was performed using the moments threshold in FIJI to determine positive signal. Droplets were further identified by watershed separation. Particle analysis was used to assess the droplets for area. Nuclear/Cytoplasmic TAZ quantification was performed in by first creating nuclear ROIs by gaussian blurring the Hoechst channel, then using the RenyiEntropy threshold with subsequent watershed segmentation and particle analysis. Moments threshold was applied to corresponding TAZ channel. Total TAZ area measured then nuclear ROIs were applied and total nuclear TAZ was measured, and finally ratio calculated. Cellular pFAK quantification was performed in FIJI by first creating cellular ROIs (10-12 cells), by splining cells. Isodata threshold was applied to pFAK channel and individual cellular pFAK area was measured. To determine the fraction of PDGFR α labeled cells that also expressed CTGF, all PDGFR α labeled cells were counted, followed by the counting of those cells that had CTGF expression.

For migration experiments, time-lapse microscopy was performed on an LSM800 laser scanning confocal microscope (Zeiss). Unless otherwise specified, migration experiments were imaged 6 h after cell seeding at 15 min frame intervals over 24 h. Immediately prior to imaging, cell nuclei were labeled with Hoechst 33342 (3 μ g/mL) for 10 min and rinsed with media for 10 min. Following raw image export, cell nuclei were tracked with a custom Matlab script described previously (14). Briefly,

parameters to threshold and locate the centroids of cell nuclei were identified and applied uniformly across the entire data set. Nuclei centroids in serial images were linked using IDL to define migration tracks. Migration speed was calculated as total tracked distance over total tracked duration. Distances were measured from the centroid of the cell nucleus at the final frame relative to the initial frame of the timelapse. Adhesion analysis was performed as described previously (15). Briefly, all samples were imaged under identical acquisition settings and thresholding for segmentation was maintained consistent across the full data set. Focal adhesions were defined as regions of vinculin fluorescence with areas $> 1 \mu\text{m}^2$.

Cell Culture

Mesenchymal progenitor cells from the HO site were harvested as previously described (16). Experiments were performed using passages 2-4. Cells were plated in regular growth medium (DMEM + 10% FBS and 1% penicillin/streptomycin). For differentiation, 1:1 osteogenic:adipogenic differentiation media was used; osteogenic differentiation medium contains 50ug/ml ascorbic acid, and 10mM beta-glycerophosphate in regular growth medium and adipogenic differentiation medium contains 5ug/mL Insulin (I3536-100MG, Sigma-Aldrich), 3uM Rosiglitazone (71740, Cayman Chemicals), 115ug/mL IBMX (13347, Cayman Chemicals), and 1uM Dexamethasone (D1756, Sigma-Aldrich). For analysis of cell morphology and focal adhesions, cells were harvested 24 hours after plating and immunocytochemistry performed. Differentiation studies were plated at 150k cells per fiber coverslip. Cells were harvested for RNA analysis on Day 3. For analysis of nuclear cytoplasmic TAZ, cells were harvested 2 days after plating and ICC was performed. For analysis of lipid droplets, cells initially received 1:1 osteogenic:adipogenic differentiation media, then changed on day 2 to modified 1:1 osteogenic:adipogenic medium (IBMX and Dexamethasone are not added) and used with subsequent medium changes every other day until collected on day 7 for ICC.

RNA Purification and RT-pPCR

Cells were harvested in TRIzol® reagent (Ambion™/Life Technologies) and extracted with chloroform. RNA was subsequently purified using RNeasy® Mini Kit reagents (74104, Qiagen™) following manufacturer's protocol supplemented with RNA mini spin column (EZCR101, Enzymax). High Capacity cDNA Reverse Transcription Kit (4364966, Applied Biosystems™) was used to convert RNA to cDNA following the manufacturer's protocol. cDNA was diluted 1:3. TaqMan® FAM-MGB primer/probe mixes were obtained from ThermoFisher Scientific™. Assays for GapdH (Mm99999915_g1), Runx2 (Mm00501584_m1), Adipoq (Mm00456425_m1) were used according to manufacturer's protocol for TaqMan® (Applied Biosystems™). Technical triplicates were performed for each gene expression assay. Plates were run on 7900HT sequence detection system following standard Taqman protocol with cycle number extended to 50. Using excel, the $\Delta\Delta C_T$ method was calculated. Biological n=3 with experimental duplicate was performed.

Statistics

Statistical analyses were performed in IBM SPSS Statistics 25 and GraphPad Prism 8. Tests for normality and heterogeneity were performed to determine appropriate statistical analysis. Student's T-test with appropriate assumptions were performed for tests comparing two groups and represented as mean with SEM significance denoted by *, (p* < 0.05, p** < 0.01, p*** < 0.001, p**** < 0.0001). Mann-Whitney Non-Parametric Comparison were performed for non-parametric data comparing two groups. Data shown as median with interquartile range and p-value represented by #, (p# < 0.05, p## < 0.01, p### < 0.001, p#### < 0.0001). ANOVA with appropriate post-hoc analysis was performed when comparing three or more groups. All analyses were two sided and performed with $\alpha=0.05$.

Bibliography:

1. Butler A, Hoffman P, Smibert P, Papalexi E, and Satija R. Integrating single-cell transcriptomic data across different conditions, technologies, and species. *Nature Biotechnology*. 2018;36:411.
2. Butler A, Hoffman P, Smibert P, Papalexi E, and Satija R. Integrating single-cell transcriptomic data across different conditions, technologies, and species. *Nat Biotechnol*. 2018;36(5):411-20.
3. Ahsan S, and Draghici S. Identifying Significantly Impacted Pathways and Putative Mechanisms with iPathwayGuide. *Curr Protoc Bioinformatics*. 2017;57:7 15 1-7 30.
4. Corces MR, Trevino AE, Hamilton EG, Greenside PG, Sinnott-Armstrong NA, Vesuna S, et al. An improved ATAC-seq protocol reduces background and enables interrogation of frozen tissues. *Nat Methods*. 2017;14(10):959-62.
5. Boyle AP, Guinney J, Crawford GE, and Furey TS. F-Seq: a feature density estimator for high-throughput sequence tags. *Bioinformatics*. 2008;24(21):2537-8.
6. Yu G, Wang LG, and He QY. ChIPseeker: an R/Bioconductor package for ChIP peak annotation, comparison and visualization. *Bioinformatics*. 2015;31(14):2382-3.
7. Trapnell C, Cacchiarelli D, Grimsby J, Pokharel P, Li S, Morse M, et al. The dynamics and regulators of cell fate decisions are revealed by pseudotemporal ordering of single cells. *Nat Biotechnol*. 2014;32(4):381-6.
8. Lowe CE, O'Rahilly S, and Rochford JJ. Adipogenesis at a glance. *Journal of cell science*. 2011;124.
9. Meyer MB, Benkusky NA, Sen B, Rubin J, and Pike JW. Epigenetic Plasticity Drives Adipogenic and Osteogenic Differentiation of Marrow-derived Mesenchymal Stem Cells. *The Journal of biological chemistry*. 2016;291(34):17829-47.
10. Ambele MA, Dessels C, Durandt C, and Pepper MS. Genome-wide analysis of gene expression during adipogenesis in human adipose-derived stromal cells reveals novel patterns of gene expression during adipocyte differentiation. *Stem Cell Res*. 2016;16(3):725-34.
11. Graneli C, Thorfve A, Ruetschi U, Brisby H, Thomsen P, Lindahl A, et al. Novel markers of osteogenic and adipogenic differentiation of human bone marrow stromal cells identified using a quantitative proteomics approach. *Stem Cell Res*. 2014;12(1):153-65.
12. Peterson JR, Okagbare PI, De La Rosa S, Cilwa KE, Perosky JE, Eboda ON, et al. Early detection of burn induced heterotopic ossification using transcutaneous Raman spectroscopy. *Bone*. 2013;54(1):28-34.
13. Schindelin J, Arganda-Carreras I, Frise E, Kaynig V, Longair M, Pietzsch T, et al. Fiji: an open-source platform for biological-image analysis. *Nat Methods*. 2012;9(7):676-82.
14. Wang WY, Davidson CD, Lin D, and Baker BM. Actomyosin contractility-dependent matrix stretch and recoil induces rapid cell migration. *Nature communications*. 2019;10(1):1186.
15. Baker BM, Trappmann B, Wang WY, Sakar MS, Kim IL, Shenoy VB, et al. Cell-mediated fibre recruitment drives extracellular matrix mechanosensing in engineered fibrillar microenvironments. *Nature materials*. 2015;14(12):1262-8.

16. Agarwal S, Drake J, Qureshi AT, Loder S, Li S, Shigemori K, et al. Characterization of Cells Isolated from Genetic and Trauma-Induced Heterotopic Ossification. *PLoS one*. 2016;11(8):e0156253.